PLOS ONE

RESEARCH ARTICLE

Stress distribution on different bar materials in implant-retained palatal obturator

Regina Furbino Villefort [1‡], **João Paulo Mendes Tribst** [2‡*], **Amanda Maria de Oliveira Dal Piva** [2©], **Alexandre Luiz Borges** [2©], **Nívia Castro Binda** [1©], **Carlos Eduardo de Almeida Ferreira** [3©], **Marco Antonio Bottino** [2©], **Sandra Lúcia Ventorim von Zeidler** [1©]

1 Biotechnology Program, Federal University of Espírito Santo, Rede Nordeste de Biotecnologia (RENORBIO), Vitória, Espírito Santo, Brazil, **2** Post-Graduate Program in Restorative Dentistry (Prosthodontic), Department of Dental Materials and Prosthodontics, Institute of Science and Technology, São Paulo State University (Unesp/SJC), São José dos Campos, SP, Brazil, **3** Private Practitioner, Vitória, Espírito Santo, Brazil

© These authors contributed equally to this work.
‡ These authors also contributed equally to this work.
* Joao.tribst@gmail.com

Abstract

Implant-retained custom-milled framework enhances the stability of palatal obturator prostheses. Therefore, to evaluate the mechanical response of implant-retained obturator prostheses with bar-clip attachment and milled bars, in three different materials under two load incidences were simulated. A maxilla model which Type IIb maxillary defect received five external hexagon implants (4.1 x 10 mm). An implant-supported palatal obturator prosthesis was simulated in three different materials: polyetheretherketone (PEEK), titanium (Ti:90%, Al:6%, V:4%) and Co-Cr (Co:60.6%, Cr:31.5%, Mo:6%) alloys. The model was imported into the analysis software and divided into a mesh composed of nodes and tetrahedral elements. Each material was assumed isotropic, elastic and homogeneous and all contacts were considered ideal. The bone was fixed and the load was applied in two different regions for each material: at the palatal face (cingulum area) of the central incisors (100 N magnitude at 45˚); and at the occlusal surface of the first left molar (150 N magnitude normal to the surface). The microstrain and von-Mises stress were selected as criteria for analysis. The posterior load showed a higher strain concentration in the posterior peri-implant tissue, near the load application side for cortical and cancellous bone, regardless the simulated material. The anterior load showed a lower strain concentration with reduced magnitude and more implants involving in the load dissipation. The stress peak was calculated during posterior loading, which 77.7 MPa in the prosthetic screws and 2,686 µε microstrain in the cortical bone. For bone tissue and bar, the material stiffness was inversely proportional to the calculated microstrain and stress. However, for the prosthetic screws and implants the PEEK showed higher stress concentration than the other materials. PEEK showed a promising behavior for the bone tissue and for the integrity of the bar and bar-clip attachments. However, the stress concentration in the prosthetic screws may represent an increase in failure risk. The use of Co-Cr alloy can reduce the stress in the prosthetic screw; however, it increases the bone strain; while the Titanium showed an intermediate behavior.

Introduction

Palatal obturator prostheses and microvascular reconstructive techniques are common treatment options for rehabilitation of those patients undergoing maxillectomy during surgical resection of tumors [1, 2]. Nevertheless, prosthetic rehabilitation remains the most widely used approach, especially for large maxillary defects [3, 4], with improvements in oral functions [5] and significant increase in the quality of life of patients [6]. The design of the obturator prosthesis and retention mechanisms depend basically on the size and location of the defect, clinical conditions of bone, remaining teeth, soft tissue, muscle control, and the physical and mental health conditions of the patient [7]. However, the retention of these prostheses for edentulous patients is often insufficient. In a systematic review on functional outcomes in oncologic patients, the authors observed that rehabilitation with implants significantly improved prosthesis retention, presenting a beneficial effect for masticatory efficiency and greater satisfaction of patients [8].

The possibility of using computer-aided design/computer-aided-manufacturing (CAD/CAM) technology to machine reliable prostheses in different materials (metal, ceramics and polymers) has diversified the standard designs of implant-supported prostheses and their clinical performance [9, 10]. Furthermore, CAD/CAM frameworks retained by implants improved the palatal obturator stability and functional results for patients with partial maxillectomy [11]. Titanium and cobalt-chromium alloys represent standard materials for CAD/CAM frameworks, with good performance and similar fit [12], while polyetheretherketone (PEEK) is an inert, non-allergenic polymeric biomaterial, indicated as a substitute for metal alloys in assorted types of prostheses and orthoses, including craniofacial prostheses [13, 14].

In vitro studies and short-term clinical reports evaluated the use of PEEK in dentistry for partial/total; fixed/removable; tooth supported/implant-supported [15–21], and maxillofacial prosthesis, including palatal obturators [22]. PEEK has shown some advantages such us the fact of it has an elastic modulus similar to the native bone, is easily obtained in personalized three-dimensional (3D) forms, propitiates the manufacture of radiolucent prostheses, with good biomechanical properties, and less accumulation of biofilm than ceramics and metallic alloys, which are usual materials in restorative dentistry [15–21]. Despite that, the biomechanical behavior of PEEK obturator prostheses retained by implants remains unknown, as well the mechanical response during chewing loads in the implants, prosthetics screws, cortical and cancellous bone for the patients rehabilitated with implant-retained obturator prostheses.

The assessment of biomechanical behavior can be performed through simulations to obtain pre-clinical data with bioengineering tools such as strain gauge, digital image correlation, photoelasticity and finite element analysis (FEA). The latter allows us to understand how the distribution of strain in bone tissue and stress in implants can be influenced by the restorative material [23], prosthesis and framework design [24, 25], manufacturing technique [26], number and distribution of implants [27–29] and attachment systems [30, 31]. Computer-assisted implant planning has become an important diagnostic and therapeutic tool in modern dentistry. The ideal implant positions can be planned virtually with the help of guided surgery software allowing for three-dimensional visualization before treatment. The combination of planning and case study by FEA can help to choose and predict the most suitable mechanical results.

Thus, the objective of this study was to evaluate the mechanical response of implant-retained obturator prostheses with bar-clip attachment and milled bars in three different materials: PEEK, titanium and cobalt-chromium alloys in different load incidences. The null hypothesis is that different materials for the framework will not modify the mechanical response in the analyzed structures regardless of the applied load.

Methods

Pre-processing

A computer tomography (CT) from São Paulo State University database, without maxillofacial abnormalities, were saved in DICOM (Digital Imaging and Communications in Medicine) format. This file comes from the University database, the authors have no access to any identifying information or taking the CT scan. The DICOM file was converted to STL (stereolithography) file in a 3D slicer software. Using CAD (computer-aided design) software (Rhinoceros Version 4.0 SR8, McNeel North America, Seattle, WA, USA), a model of an edentulous maxilla was constructed following the main anatomical characteristics of the patient's bone: size, shape and absence of lesion. The next step was to reconstruct the NURBS (non-uniform rational B-spline) surfaces from mesh with precision. For that, the BioCAD method [32] was applied and the anatomical lines of the surface were created. The pre-processing phase is summarized in a flowchart (Fig 1). The 3D volumetric model of the bone was then finished based on the surface created by the curve network manually generated (Fig 2A). The cortical bone (Fig 2E) contained 1 mm thickness in juxtaposition with cancellous bone (Fig 2D) [33]. The command offset surface was used to create the soft tissue with 2 mm thickness [34] (Fig 2F).

External hexagon implants (10 × 4.1 mm), previously modeled [25] were selected. The platform had a diameter of 4.1 mm, similar to a regular conventional implant. The external hexagon was extruded (0.7 mm high) and attached to the previously created cylindrical body [33] (Fig 2H). The minimum distance between the implants was 4 mm (Fig 2G). The prosthetic screw was modeled for each implant (Fig 2I). The total number of implants and their position were based in a previous report with the similar prosthetic approach [11] (Fig 2B). After that Type IIb defect [35] was simulated following the length and width from a clinical report [36] (Fig 2B).

The bar was modeled following the maxilla shape and the implants position. It presents 3 mm maximum thickness and 4 mm width, rounded corners and flat surfaces. An anteroposterior structure was used crossing the hemimaxillectomy defects similar to [11] report (Fig 3).

After that, the full-arch total prosthesis was modeled containing artificial teeth [33] and palatal coverage (Fig 2J). The clip connector for the fixture system was modeled in the same position as the bar from the framework.

Processing

For the FEA, each solid geometry was imported to the computer aided engineering (CAE) software (ANSYS 19.2, ANSYS Inc., Houston, TX, USA) in STEP format. A 3D mesh was generated, and tetrahedral elements were considered for the models. A convergence test (maximum of 10% of difference in results between each calculation) determined the total number of elements (169,546) and nodes (306,914) for the model (Fig 4A). The Elastic modulus and Poisson ratio of each material were assigned to each solid component with isotropic and homogeneous behavior (Table 1). The contacts were considered perfectly bonded between the structures.

For the boundary conditions, the bottom surface of cancellous bone was restricted in all directions Fig 4B). Wedel et al. [44] established 120N as the occlusal force in patients with congenital and acquired maxillofacial defects while another studies reported the load range of 48–300 N for overdenture patients [45–47]. In this study, both simulated loads are inside this range.

The load was applied in two different moments for each material: at the palatal face (cingulum area) of the central incisors with 100 N magnitude applied at 45° [48] (Fig 4C); and at the occlusal surface of the first left molar with 150 N magnitude applied normal to the surface [29] (Fig 4D).
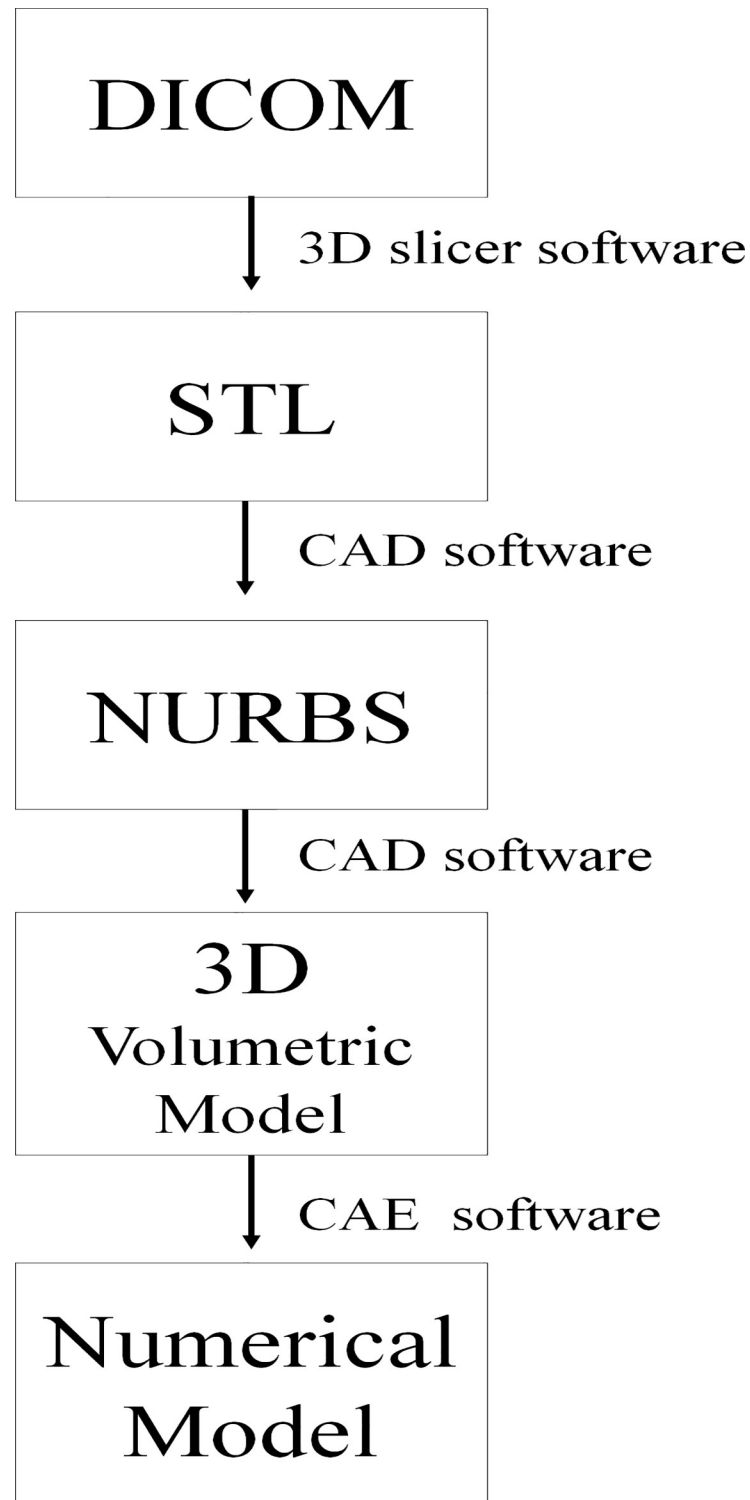
Fig 1. Process flowchart. Diagrammatic representation of the steps and the correlated software applied in the pre-processing and processing phases.

https://doi.org/10.1371/journal.pone.0241589.g001

Fig 2. 3D model and geometries. Edentulous maxilla (A); Type IIb maxillary defect (B); Implants distribution on maxillary crestal bone (C); Cancellous bone (D); Cortical bone (E); Soft tissue (F); Five external hexagon implants (G); Bar and bar-clip attachments (H); Five prosthetic screws (I); Full-arch total prosthesis (J).
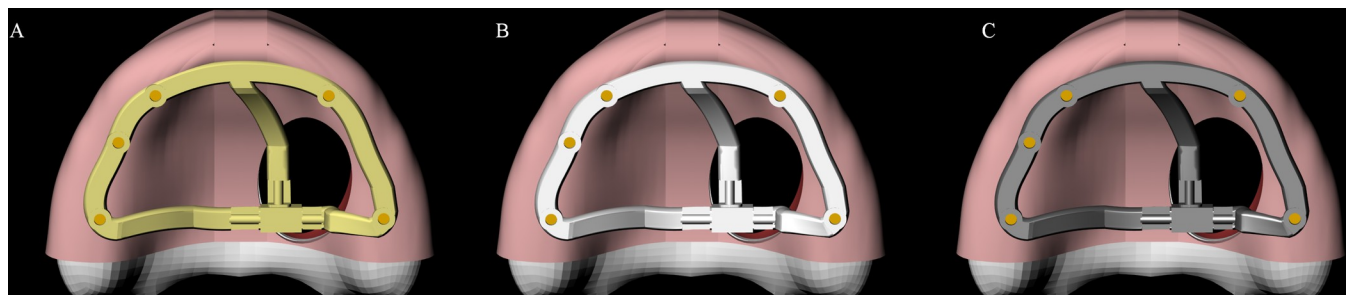
https://doi.org/10.1371/journal.pone.0241589.g002

Fig 3. 3D model. Milled implant-retained bar with 3 clip-bar attachments in different materials. PEEK (A); Titanium alloy (B); Cobalt-Chromium alloy (C).

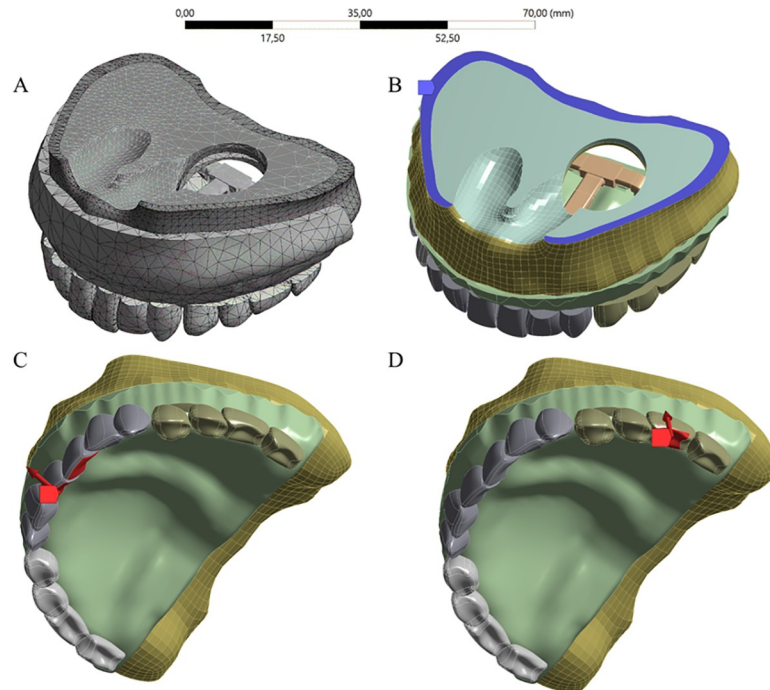https://doi.org/10.1371/journal.pone.0241589.g003

Fig 4. Boundary conditions and loadings configuration in FEA models. Mesh (A); Boundary conditions (B); Anterior load was applied at cingulum area of the central incisor (C); Posterior load was applied at occlusal surface of the first molar (D).

https://doi.org/10.1371/journal.pone.0241589.g004

Results were reported in von Mises stress [25] distribution for the framework, implants and screw; and in microstrains (με) for bone tissue [49].

Results

The calculated microstrain distribution in the maxilla as a function of the framework's material and load incidence were plotted in colorimetric graphs in the Figs 5 and 6 for cortical and cancellous bone, respectively. It was possible to observe that the posterior load showed a higher strain concentration in the posterior peri-implant tissue, near the load application side for cortical and cancellous bone. The anterior load showed a lower strain concentration with reduced magnitude and more implants involving in the load dissipation.

Moreover, the higher the framework elastic modulus, the higher the bone strain regardless the evaluated bone tissue and load incidence. The peak value of each group was exported from the analysis software to quantify the strain (Table 2). According to Wolff's law, strain values

Table 1. Mechanical properties of the materials/solid geometry used in the current study.

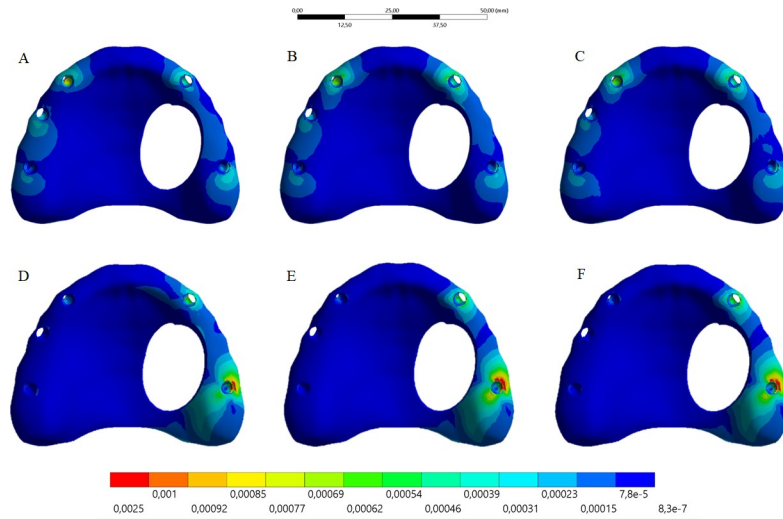| Material/solid geometry	Young's Modulus (GPa)	Poisson Ratio
Cancellous bone [37]	1.37	0.3
Cortical bone [38]	14.7	0.3
Soft tissue [39]	0.68	0.45
PEEK [40]	3.7	0.4
Titanium alloy [41]	110	0.3
Cobalt-Chromium alloy [42]	200	0.3
Acrylic resin [43]	2.83	0.45

https://doi.org/10.1371/journal.pone.0241589.t001

Fig 5. Microstrain distribution in the maxillary cancellous bone. Upper line: anterior loading; Bottom line: posterior loading. Framework's material: PEEK (A and D); Titanium alloy (B and E); Cobalt-Chromium alloy (C and F).

below 50 mm/mm are able to promote bone remodeling by disuse, and those values above 3000 mm/mm are able to promote bone remodeling by micro-damage. Thus, the three types of framework's material showed no values able to induce an unwanted bone remodeling.

The stress distribution in the framework for all groups is displayed in the Fig 7. Similar to the bone tissue mechanical behavior, the higher the framework elastic modulus, the higher the stress concentration regardless the load incidence. For posterior load, the stress concentration occurred in the lateral side; and for the anterior load, the stress concentration occurred between the anterior implants, near the screw access holes.

A higher stress concentration in the framework promoted a lower stress concentration in the implant (Figs 8 and 9) and prosthetic screw (Figs 10 and 11). Observing the results displayed in the Fig 9 it is possible to see that the higher the framework elastic modulus, the lower
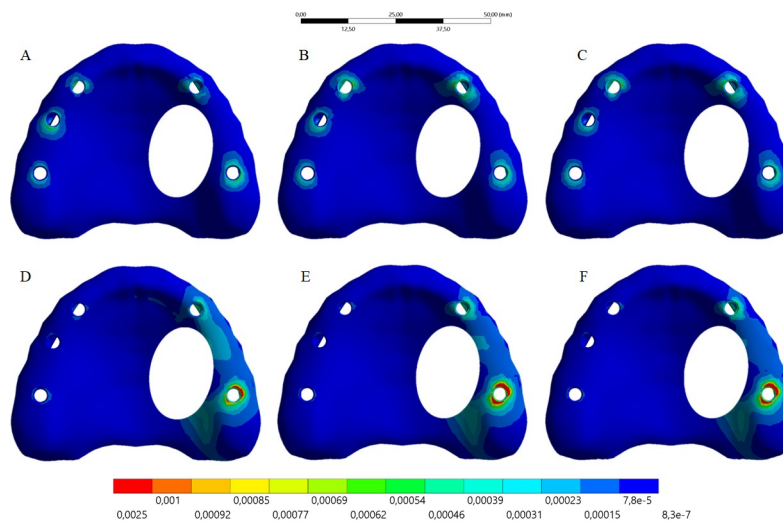

Fig 6. Microstrain distribution on the maxillary cortical bone. Upper line: anterior loading; Bottom line: posterior loading. Framework's material: PEEK (A and D); Titanium alloy (B and E); Cobalt-Chromium alloy (C and F).

Table 2. Results in terms of bone microstrain (με) and stress peak values (MPa) according to the framework's material and load incidence.

	PEEK		Titanium		CoCr	
	Anterior	Posterior	Anterior	Posterior	Anterior	Posterior
Cortical Bone (με)	411	1,460	460	2,360	492	2,686
Cancellous Bone (με)	588	1,258	567	1,896	587	1,987
Framework (MPa)	4.6	9.5	66.3	51.4	71.7	62.5
Implant (MPa)	25.4	86.4	20.8	79.2	19.8	74.1
Prosthetic Screw (MPa)	53.2	77.7	22.6	40.3	22.1	25.3

the stress concentration in the implants. The posterior load showed a higher stress magnitude with more red fringes in the colorimetric stress map in comparison with the anterior load, with the most posterior implant being the most affected. For the prosthetic screw, the same stress pattern observed in the implants occurred (Fig 11). The highest stress concentration calculated for the screw is the combination of PEEK framework and posterior load.

The results in terms of stress peak values (MPa) in the framework, prosthetic screw, and implant are summarized in Table 2.

Discussion

This study aimed to evaluate the mechanical response of implant-retained obturator prostheses with clip-bar system, in different materials. The hypothesis was rejected due to the differences of stress concentration observed among materials.

Technical and biological complications or even failures are usual outcomes in dental prosthesis and it should be considered, in order to prevent them. Biomechanical tests are consolidated methods which have been contributing to the comprehension of the behavior of restorative materials and this study compared the mechanical response of CoCr and titanium alloys (materials commonly used for CAD/CAM frameworks) with the PEEK, an alternative to metal alloys in dentistry. The elastic modulus of Co-Cr alloy (200 GPa) [42] is almost double of the titanium's modulus (110 GPa) [41] and both have the same Poisson coefficient, while PEEK presents both, elastic modulus and Poisson coefficient, closer to those of acrylic resin
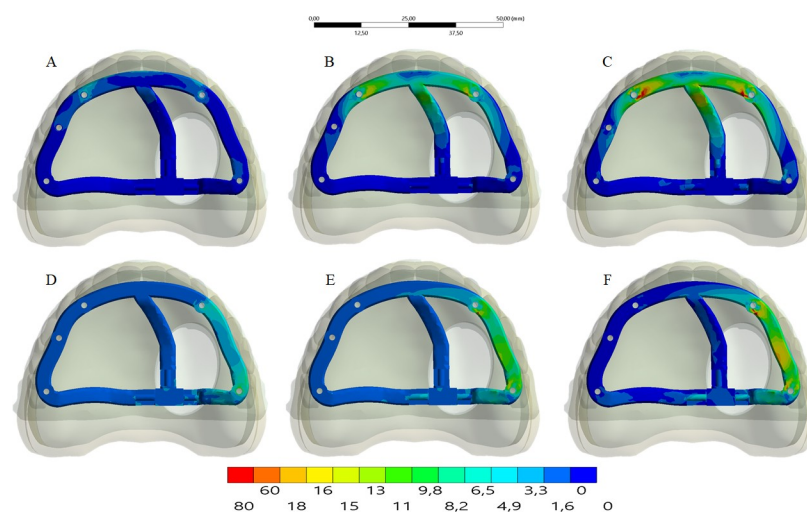

Fig 7. The stress distribution in the framework. Upper line: anterior loading; Bottom line: posterior loading. Framework's material: PEEK (A and D); Titanium alloy (B and E); Cobalt-Chromium alloy (C and F).
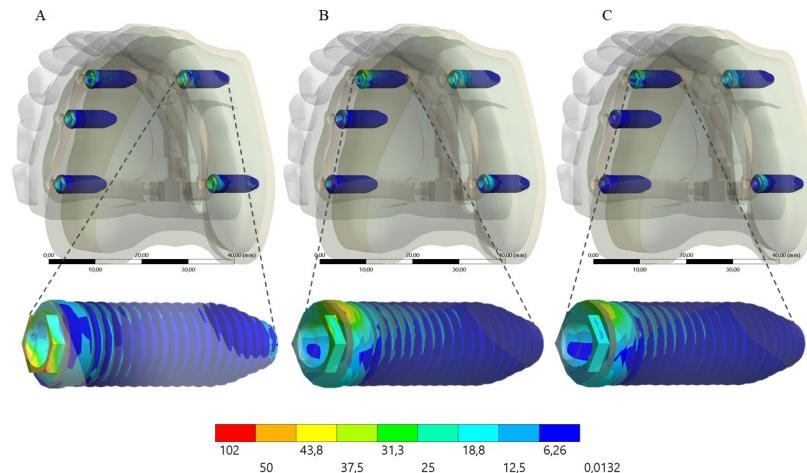
Fig 8. Maps of von Mises stress distribution results for implants according to framework's material, under anterior loading. PEEK (A); Titanium (B); Cobalt-Chromium alloy (C). On the bottom line, an enlarged view of the implants that presented the highest stress concentration.

https://doi.org/10.1371/journal.pone.0241589.g008

[43] (material used in synthetic teeth). This difference makes the metal alloys behave differently from the PEEK when the anterior and posterior loads are applied. Therefore, the higher stress concentration was calculated in the CoCr bar, followed by titanium and finally the PEEK bar.

According to Bhering et al. [50], rigid frameworks transmit lower load to the implant and prosthetic components, when compared to the less rigid ones. Nonetheless, variations of framework material rigidity did not demonstrate a significant effect on the stress values in the marginal bone around the implants [51] and Medeiros et al. [26] observed that the occlusal coating had a greater influence on the load dissipations than the framework. In consonance with Erkmen et al. [52] the current study demonstrated that by using less rigid material for milled bar in implant-retained prostheses the stresses within both, the framework and the veneering parts, decreased due to the flexible nature of the material that absorbs stresses. The
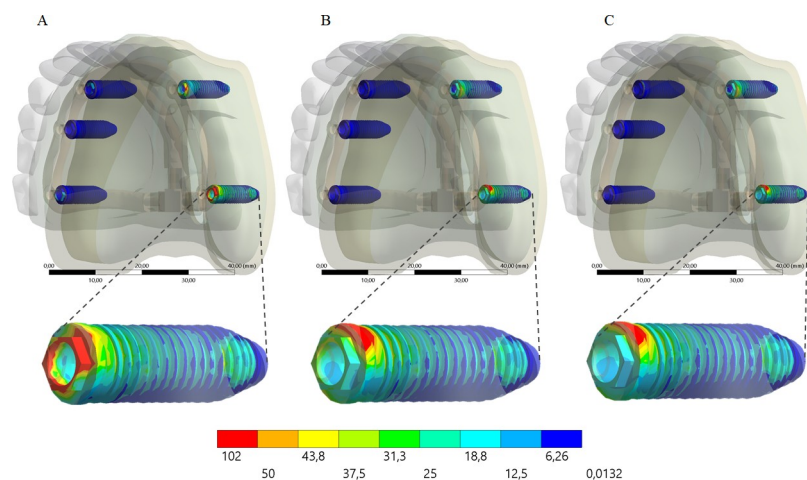

Fig 9. Maps of von Mises stress distribution results for implants according to framework's material, under posterior loading. PEEK (A); Titanium (B); Cobalt-Chromium alloy (C). On the bottom line, an enlarged view of the implants that presented the highest stress concentration.
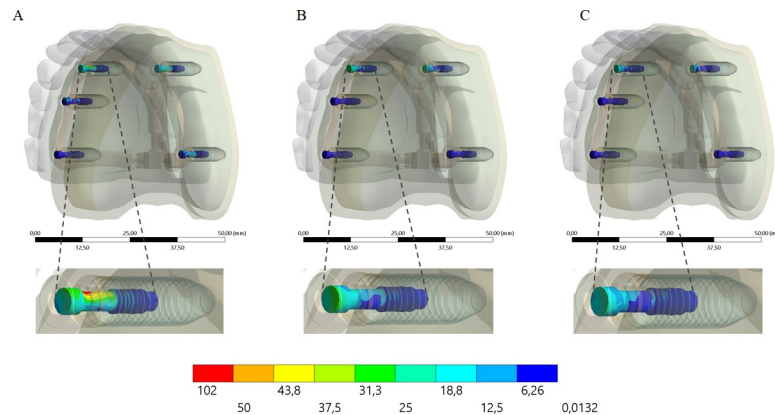
https://doi.org/10.1371/journal.pone.0241589.g009

Fig 10. Maps of von Mises stress distribution results for prosthetic screw according to framework's material, under anterior loading. PEEK (A); Titanium alloy (B); Cobalt-Chromium alloy (C). On the bottom line, an enlarged view of the prosthetic screws that presented the highest stress concentration.

results from a longitudinal study on the use of PEEK milled bar as framework for implant-supported full-arch fixed prostheses suggest that this material may become an appropriate treatment option [21].

Apart from the material, the custom-milled framework design also influences the stress distribution [25]. In conventional maxillary overdentures that do not require palatal coverage, the stresses tend to be concentrated in the distal of the last implant, in the cantilever region [30]. However, obturator prostheses aims both coverage and adequate sealing of the oroantral communication, and thus the cantilever ceases to exist if there is residual bone on the affected side, or if zygomatic implants are installed. The maximum displacement of the obturator prosthesis increases as less residual bone is present, as well as less implants and clips [53]. Therefore, the unaffected side by maxillectomy should receive a larger number of implants to reduce the stress concentration in the framework [27]. The present study evaluated the performance of a milled bar for obturator prosthesis with polygonal geometry, without cantilever and with total palatal coverage and three clips in the region of the maxillary defect, supported by five implants. This model was based on a clinical case [36] and it was observed that despite the number of implants at unaffected side, the unilateral posterior loading promoted higher stress
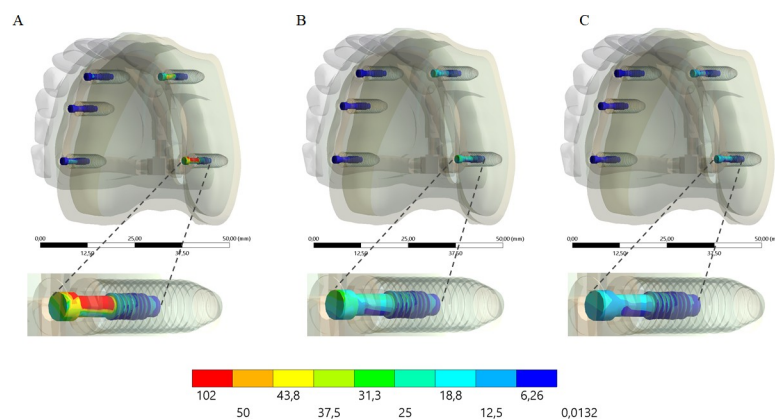

Fig 11. Maps of von Mises stress distribution results for prosthetic screw according to framework's material, under posterior loading. PEEK (A); Titanium alloy (B); Cobalt-Chromium alloy (C). On the bottom line, an enlarged view of the prosthetic screws that presented the highest stress concentration.

concentration in the mesial buccal and distal palatal portions of the cervical bone (cancellous and cortical) on the most distal implant on the affected side.

Regarding to the anchorage system, bar-clips possess a more favorable design to distribute the loads than O-rings [54] and presents lower strain values when submitted to compressive occlusal loads [55]. Furthermore, this system had a better biomechanical performance with the lowest strain values around the dental implants when subjected to forces simulating prosthesis removal [56]. In the current study, three the bar-clips were simulated in different materials and it was observed that PEEK attachments concentrated less stress than the metallic ones. This could be consider a possible advantage of using PEEK, taking into account that according to Tanoue et al. [57] clips can prevent the fracture of the prosthesis base more than metal clips, regardless of the number, due the lower concentration of stress observed around plastic clips. However, it is important to emphasize that the most frequent complication in implant-supported overdentures with bar-clip system are associated with the retention clips, requiring its replacement in 33% of cases [58].

For implant-supported rehabilitation, the marginal bone loss with exposure of the implant threads can be considered one of the biological complications. Frost [49] suggests that unrepaired bone resorption starts when strains exceed 3000μ strain. In the present study, the use of PEEK milled bar suggests a better mechanical performance for bone tissue with less possibility of unwanted bone resorption due to less peri-implant deformation independent on the simulated masticatory load.

Stress concentration on prosthetic screws is influenced by implant connection and the material selected for abutments and frameworks. Less rigid abutments like those manufactured in reinforced fiber composite and PEEK are not absolutely relevant for morse-taper implant [59]. In contrast, for external hexagon implants, flexible prosthetic frameworks increases the stress generated in the prosthetic screw threads [23] and may decrease the survival of restorations under cyclic fatigue [60]. This is relevant because abutment screw loosening, the fixing screw fractures, screw retightening and loosening of the abutment are usual technical complications in implant-retained prosthesis. Thus, the results of the present study suggest that the use of PEEK might facilitate the emergence of mechanical complications in prosthetic screws compared with metal frameworks.

Inherent limitations of the finite element analysis studies and biologic simulations were observed in the present investigation and two assumptions figured as the principals. The first one was the simulated materials presented a homogeneous structure and linearly isotropic behavior that do not represent the defects population incorporated during the prosthesis manufacturing. The second was that the implants were assumed 100% osseointegrated, although histomorphometric studies indicated that there is not a 100% bone–implant interface. Nonetheless, these assumptions are consistent with other FEA studies [29, 50, 52] and are consequences of the challenges in establishing the properties of living tissues and the osseointegration level in bone-implant surfaces. Furthermore, it would not interfere with the qualitative and comparative results because they were present for all models. Future fatigue life studies and clinical evaluations may complement the results or evaluating the different framework materials described for this technique.

Conclusion

For this treatment modality, regardless the loading region, PEEK can be suggested as framework material to reduce the bone strain around the implants and the stress concentration in the bar structure. However, the use of PEEK increase the risk of prosthetic screws loosening and even fracture in comparison with metallic alloys.

Author Contributions

References

1. Vander Poorten V, Meulemans J, Delaere P. Midface prosthetic rehabilitation. Current Opinion in Otolaryngology and Head and Neck Surgery. 2016. pp. 98–109. https://doi.org/10.1097/MOO.0000000000000241 PMID: 26785170

2. Park J-H, Lee K-S, Lee J-Y, Shin S-W. Fabricating a Maxillary Obturator Using an Intraoral Digital Impression: A Case History Report. Int J Prosthodont. 2017; 30: 266–268. https://doi.org/10.11607/ijp.5213 PMID: 28453002

3. Sakuraba Minoru, Kimata Yoshihiro, Ota Yojiro, Uchiyama Kiyotaka, Kishimoto Seiji, Kiyonori Harii SE. Simple maxillary reconstruction using free tissue transfer and prostheses. Plast Reconstr Surg. 2003; 2: 594–8.

4. Moreno MA, Skoracki RJ, Hanna EY HM. Microvascular free flap reconstruction versus palatal obturation for maxillectomy defects. Head Neck. 2010; 32: 860–868. https://doi.org/10.1002/hed.21264 PMID: 19902543

5. Chen C, Ren W, Gao L, Cheng Z, Zhang L, Li S, et al. Function of obturator prosthesis after maxillectomy and prosthetic obturator rehabilitation. Braz J Otorhinolaryngol. 2016; 82: 177–183. https://doi.org/10.1016/j.bjorl.2015.10.006 PMID: 26671022

6. Artopoulou II, Karademas EC, Papadogeorgakis N, Papathanasiou I, Polyzois G. Effects of sociodemographic, treatment variables, and medical characteristics on quality of life of patients with maxillectomy restored with obturator prostheses. J Prosthet Dent. 2017; 118: 783–789.e4. https://doi.org/10.1016/j.prosdent.2017.01.021 PMID: 28456369

7. Gastaldi G, Palumbo L, Moreschi C, Gherlone EF CP. Prosthetic management of patients with oro-maxillo-facial defects: a long-term follow-up retrospective study. Oral Implant. 2017; 10: 276–282. https://doi.org/10.11138/orl/2017.10.3.276 PMID: 29285330

8. Said MM, Otomaru T, Sumita Y, Leung KCM, Khan Z, Taniguchi H. Systematic review of literature: functional outcomes of implant-prosthetic treatment in patients with surgical resection for oral cavity tumors. J Investig Clin Dent. 2017; 8: 1–9. https://doi.org/10.1111/jicd.12207 PMID: 26749088

9. Harder S, Kern M. Survival and complications of computer aided-designing and computer-aided manufacturing vs. conventionally fabricated implant-supported reconstructions: A systematic review. Clin Oral Implants Res. 2009; 20: 48–54. https://doi.org/10.1111/j.1600-0501.2009.01778.x PMID: 19663948

10. Oh J. Recent advances in the reconstruction of cranio-maxillofacial defects using computer-aided design/computer-aided manufacturing. Maxillofac Plast Reconstr Surg. 2018;40. https://doi.org/10.1186/s40902-018-0179-8 PMID: 30591916

11. Mertens C, de San Jose Gonzalez J, Freudlsperger C, Bodem J, Krisam J, Hoffmann J, et al. Implant-prosthetic rehabilitation of hemimaxillectomy defects with CAD/CAM suprastructures. J Cranio-Maxillofacial Surg. 2016; 44: 1812–1818. https://doi.org/10.1016/j.jcms.2016.08.009 PMID: 27663677

12. Svanborg P, Stenport V, Eliasson A. Fit of cobalt–chromium implant frameworks before and after ceramic veneering in comparison with CNC-milled titanium frameworks. Clin Exp Dent Res. 2015; 1: 49–56. https://doi.org/10.1002/cre2.9 PMID: 29744140

13. Alonso-Rodriguez E, Cebrián JL, Nieto MJ, Del Castillo JL, Hernández-Godoy J BM. Polyetheretherketone custom-made implants for craniofacial defects: Report of 14 cases and review of the literature. J Craniomaxillofac Surg. 2015; 43: 1232–1238. https://doi.org/10.1016/j.jcms.2015.04.028 PMID: 26032759

14. Zanotti B, Zingaretti N, Verlicchi A, Robiony M, Alfieri A PP. Cranioplasty: Review of Materials. J Craniofac Surg. 2016; 27: 2061–2072. https://doi.org/10.1097/SCS.0000000000003025 PMID: 28005754

15. Tetelman ED, Babbush CA. A new transitional abutment for immediate aesthetics and function. Implant Dent. 2008; 17: 51–58. https://doi.org/10.1097/ID.0b013e318167648c PMID: 18332758

16. Bayer S, Komor N, Kramer A, Albrecht D, Mericske-Stern R, Enkling N. Retention force of plastic clips on implant bars: A randomized controlled trial. Clin Oral Implants Res. 2012; 23: 1377–1384. https://doi.org/10.1111/j.1600-0501.2011.02312.x PMID: 22092547

17. Zoidis P, Papathanasiou I PG. The Use of a modified poly-ether-ether-ketone (PEEK) as an alternative framework material for removable dental prostheses. J Prosthodont. 2016; 25: 580–584. https://doi.org/10.1111/jopr.12325 PMID: 26216668

18. Stock V, Wagner C, Merk S, Roos M, Schmidlin PR, Eichberger M, et al. Retention force of differently fabricated telescopic PEEK crowns with different tapers. Dent Mater J. 2016; 35: 594–600. https://doi.org/10.4012/dmj.2015-249 PMID: 27477224

19. Andrikopoulou E, Zoidis P, Artopoulou II DA. Modified PEEK resin bonded fixed dental prosthesis for a young cleft lip and palate patient. J Esthet Restor Dent. 2016; 28: 201–207. https://doi.org/10.1111/jerd.12221 PMID: 27273727

20. Zoidis P, Bakiri E PG. Using modified polyetheretherketone (PEEK) as an alternative material for endocrown restorations: A short-term clinical report. J Prosthet Dent. 2017; 117: 335–339. https://doi.org/10.1016/j.prosdent.2016.08.009 PMID: 27692583

21. Maló P, de Araújo Nobre M, Moura Guedes C, et al. Short-term report of an ongoing prospective cohort study evaluating the outcome of full-arch implant-supported fixed hybrid polyetheretherketone-acrylic resin prostheses and the All-on-Four concept. Clin Implant Dent Relat Res. 2018; 20: 692–702. https://doi.org/10.1111/cid.12662 PMID: 30110132

22. Costa-Palau S, Torrents-Nicolas J, Brufau-De Barberà M, Cabratosa-Termes J. Use of polyetheretherketone in the fabrication of a maxillary obturator prosthesis: A clinical report. J Prosthet Dent. 2014; 112: 680–682. https://doi.org/10.1016/j.prosdent.2013.10.026 PMID: 24630397

23. Datte CE, Tribst JPM, Dal Piva AM de O, Nishioka RS, Bottino MA, Evangelhista ADM, et al. Influence of different restorative materials on the stress distribution in dental implants. J Clin Exp Dent. 2018; 10: e439–e444. https://doi.org/10.4317/jced.54554 PMID: 29849967

24. Miyashita ER, Mattos BSC, Noritomi PY, Navarro H. Finite element analysis of maxillary bone stress caused by Aramany Class IV obturator prostheses. J Prosthet Dent. 2012; 107: 336–342. https://doi.org/10.1016/S0022-3913(12)60086-9 PMID: 22546312

25. Tribst JPM, Dal Piva AM de O, Lo Giudice R, Borges ALS, Bottino MA, Epifania E, et al. The Influence of Custom-Milled Framework Design for an Implant-Supported Full-Arch Fixed Dental Prosthesis: 3D-FEA Sudy. Int J Environ Res Public Health. 2020; 17. https://doi.org/10.3390/ijerph17114040 PMID: 32517097

26. de Medeiros RA, dos Santos DM, Pesqueira AA, Campaner M, Bitencourt SB, da Silva EVF, et al. Stress distribution in fixed mandibular prostheses fabricated by CAD/CAM and conventional techniques: Photoelastic and strain gauge analyses. J Clin Exp Dent. 2019; 11: e807–e813. https://doi.org/10.4317/jced.56067 PMID: 31636873

27. Miyamoto S, Ujigawa K, Kizu Y, Tonogi M YG. Biomechanical three-dimensional finite-element analysis of maxillary prostheses with implants. Design of number and position of implants for maxillary prostheses after hemimaxillectomy. Int J Oral Maxillofac Surg. 2010; 39: 1120–1126. https://doi.org/10.1016/j.ijom.2010.06.011 PMID: 20627226

28. Akay C, Yaluğ S. Biomechanical 3-dimensional finite element analysis of obturator protheses retained with zygomatic and dental implants in maxillary defects. Med Sci Monit. 2015; 21: 604–611. https://doi.org/10.12659/MSM.892680 PMID: 25714086

29. Alvarez-Arenal A, Gonzalez-Gonzalez I, de Llanos-Lanchares H, Martin-Fernandez E, Brizuela-Velasco A, Ellacuria-Echebarria J. Effect of implant- and occlusal load location on stress distribution in Locator attachments of mandibular overdenture. A finite element study. J Adv Prosthodont. 2017; 9: 371–380. https://doi.org/10.4047/jap.2017.9.5.371 PMID: 29142645

30. Kim MJ, Hong SO. Finite element analysis on stress distribution of maxillary implant-retained overdentures depending on the Bar attachment design and palatal coverage. J Adv Prosthodont. 2016; 8: 85–93. https://doi.org/10.4047/jap.2016.8.2.85 PMID: 27141251

31. Shishesaz M, Ahmadzadeh A, Baharan A. Finite element study of three different treatment designs of a mandibular three implant-retained overdenture. Lat Am J Solids Struct. 2016; 13: 2826–2844. https://doi.org/10.1590/1679-78253212

32. Kemmoku DT, Laureti CAR, Noritomi PY SJ. BioCAD techniques: Example on maxilla for rapid expansion simulation. Innovative Developments in Virtual and Physical Prototyping Y. Proceedings of the 5th International Conference on Advanced Research and Rapid Prototyping. 2012. doi:https://doi.org/10.1201/b11341-113

33. Tribst JPM, de Oliveira Dal Piva AM, Borges ALS, Rodrigues VA, Bottino MA, Kleverlaan CJ. Does the prosthesis weight matter? 3D finite element analysis of a fixed implant-supported prosthesis at different weights and implant numbers. J Adv Prosthodont. 2020; 12: 67–74. https://doi.org/10.4047/jap.2020.12.2.67 PMID: 32377319

34. Butnaru-Moldoveanu SA, Munteanu F, Forna NC. Virtual bone augmentation in atrophic mandible to assess optimal implant-prosthetic rehabilitation-A finite element study. Appl Sci. 2020; 10. https://doi.org/10.3390/app10031192 PMID: 32133203

35. Brown JS, Shaw RJ. Reconstruction of the maxilla and midface: Introducing a new classification. Lancet Oncol. 2010; 11: 1001–1008. https://doi.org/10.1016/S1470-2045(10)70113-3 PMID: 20932492

36. Domingues JM, Corrêa G, Fernandes Filho RB, Hosni ES. Palatal obturator prosthesis: case series. RGO—Rev Gaúcha Odontol. 2016; 64: 477–483. https://doi.org/10.1590/1981-863720160003000183177

37. Monteiro JB, Dal Piva AM de O, Tribst JPM, Borges ALS, Tango RN. The effect of resection angle on stress distribution after root-end surgery. Iran Endod J. 2018; 13: 188–194. https://doi.org/10.22037/iej.v13i2.19089 PMID: 29707013

38. Moroi HH, Okimoto K, Moroi R TY. Numeric approach to the biomechanical analysis of thermal effects in coated implants. Int J Prosthodont. 1993; 6: 564–572. PMID: 8148028

39. Rees JS, Huggett R HA. Finite element analysis of the stress-concentrating effect of fraenal notches in complete dentures. Int J Prosthodont. 1990; 3: 238–240. PMID: 2083009

40. Vadapalli S, Sairyo K, Goel VK et al. Biomechanical rationale for using polyetheretherketone (PEEK) spacers for lumbar interbody fusion-A finite element study. Spine (Phila Pa 1976). 2006; 31: E992–E998. https://doi.org/10.1097/01.brs.0000250177.84168.ba PMID: 17172990

41. Elias CN, Fernandes DJ, Souza FM De, Monteiro EDS, Biasi RS De. Mechanical and clinical properties of titanium and titanium-based alloys (Ti G2, Ti G4 cold worked nanostructured and Ti G5) for biomedical applications. J Mater Res Technol. 2019; 8: 1060–1069. https://doi.org/10.1016/j.jmrt.2018.07.016

42. Suleiman SH V von SP. Fracture strength of porcelain fused to metal crowns made of cast, milled or laser-sintered cobalt-chromium. Acta Odontol Scand. 2013; 71: 1280–1289. https://doi.org/10.3109/00016357.2012.757650 PMID: 23320554

43. Peyton FA CR. Current evaluation of plastics in crown and bridge prosthesis. J Prosthet Dent. 1963; 13: 745–753.

44. Wedel A, Yontchev E, Carlsson GE OR. Masticatory function in patients with congenital and acquired maxillofacial defects. J Prosthet Dent. 1994; 72: 303–308. https://doi.org/10.1016/0022-3913(94)90344-1 PMID: 7965904

45. Jemt T, Book K KS. Occlusal force and mandibular movements in patients with removable overdentures and fixed prostheses supported by implants in the maxilla. Int J Oral Maxillofac Implant. 1993; 8: 301–308. PMID: 8225465

46. Mericske-Stern R, Venetz E, Fahrländer F BW. In vivo force measurements on maxillary implants supporting a fixed prosthesis or an overdenture: a pilot study. J Prosthet Dent. 2000; 84: 535–547. https://doi.org/10.1067/mpr.2000.110264 PMID: 11105009

47. Siegele D SU. Numerical investigations of the influence of implant shape on stress distribution in the jaw bone. Int J Oral Maxillofac Implant. 1989; 4: 333–340. PMID: 2639862

48. Dal Piva AMO, Tribst JPM, Souza ROAE BA. Influence of Alveolar Bone Loss and Cement Layer Thickness on the Biomechanical Behavior of Endodontically Treated Maxillary Incisors: A 3-dimensional Finite Element Analysis. J Endod. 2017; 43: 791–795. https://doi.org/10.1016/j.joen.2016.11.020 PMID: 28343925

49. Frost HM. A 2003 update of bone physiology and Wolff s law for clinicians. Angle Orthod. 2004; 74: 3–15. https://doi.org/10.1043/0003-3219(2004)074<0003:AUOBPA>2.0.CO;2 PMID: 15038485

50. Bhering CLB, Mesquita MF, Kemmoku DT, Noritomi PY, Consani RLX, Barão VAR. Comparison between all-on-four and all-on-six treatment concepts and framework material on stress distribution in atrophic maxilla: A prototyping guided 3D-FEA study. Mater Sci Eng C. 2016; 69: 715–725. https://doi.org/10.1016/j.msec.2016.07.059 PMID: 27612765

51. Ferreira MB, Barão VA, Faverani LP, Hipólito AC, Assunção WG. The role of superstructure material on the stress distribution in mandibular full-arch implant-supported fixed dentures. A CT-based 3D-FEA. Mater Sci Eng C. 2014; 35: 92–99. https://doi.org/10.1016/j.msec.2013.10.022 PMID: 24411356

52. Erkmen E, Meriç G, Kurt A, Tunç Y, Eser A. Biomechanical comparison of implant retained fixed partial dentures with fiber reinforced composite versus conventional metal frameworks: A 3D FEA study. J Mech Behav Biomed Mater. 2011; 4: 107–116. https://doi.org/10.1016/j.jmbbm.2010.09.011 PMID: 21094484

53. De Sousa AA, Mattos BSC. Finite element analysis of stability and functional stress with implant-supported maxillary obturator prostheses. J Prosthet Dent. 2014; 112: 1578–1584. https://doi.org/10.1016/j.prosdent.2014.06.020 PMID: 25277029

54. Vafaei F, Khoshhal M, Bayat-Movahed S, et al. Comparative stress distribution of implant-retained mandibular ball-supported and bar-supported overlay dentures: a finite element analysis. J Oral Implant. 2011; 37: 421–429. https://doi.org/10.1563/AAID-JOI-D-10-00057 PMID: 20712443

55. Fanuscu MI CA. Influence of attachment systems on load transfer of an implant-assisted maxillary overdenture. J Prosthodont. 2004; 13: 214–220. https://doi.org/10.1111/j.1532-849X.2004.04041.x PMID: 15610541

56. Goiato MC, Matheus HR, de Medeiros RA, dos Santos DM, Bitencourt SB, Pesqueira AA. A photoelastic and strain gauge comparison of two attachments for obturator prostheses. J Prosthet Dent. 2017; 117: 685–689. https://doi.org/10.1016/j.prosdent.2016.07.025 PMID: 27881311

57. Tanoue M, Kanazawa M, Takeshita S, Minakuchi S. Effects of clip materials on stress distribution to maxillary implant overdentures with bar attachments. J Prosthet Dent. 2016; 115: 283–289. https://doi.org/10.1016/j.prosdent.2015.07.017 PMID: 26518988

58. Cakarer S, Can T, Yaltirik M, Keskin C. Complications associated with the ball, bar and locator attachments for implant-supported overdentures. Med Oral Patol Oral Cir Bucal. 2011; 16. https://doi.org/10.4317/medoral.17312 PMID: 21743398

59. Tretto PHW, dos Santos MBF, Spazzin AO, Pereira GKR, Bacchi A. Assessment of stress/strain in dental implants and abutments of alternative materials compared to conventional titanium alloy—3D non-linear finite element analysis. Comput Methods Biomech Biomed Engin. 2020; 23: 372–383. https://doi.org/10.1080/10255842.2020.1731481 PMID: 32116034

60. Rodrigues VA, Dal Piva AM de O, Yamaguchi CA, Borges ALS, Mukai MK, Tribst JPM. Effect of framework type on survival probability of implant-supported temporary crowns: An in vitro study. J Clin Exp Dent. 2020; 12: e433–e439. https://doi.org/10.4317/jced.56292 PMID: 32509224